Final Report
Contract F6170894 C0011
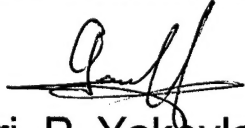
Mid-infrared diode lasers
based on III-V alloys
for the spectral range 3-3.5 μm
operating near room temperature

Phase 1
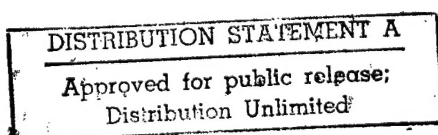### (July 1, 1994 — June 30, 1995)

The creation and studying of the lasers based on InAsSbP/InAsSb for the spectral range 3.0-3.5 μm with improved optical and electron confinements

PROJECT MANAGER: Yuri P. Yakovlev, Dr. Sci.
head of infrared optoelectronics laboratory

Ioffe Physical Technical Institute
Russian Academy of Sciences,
St. Petersburg Russia

AQ F99-05-0855

REPORT DOCUMENTATION PAGE

Form Approved OMB No. 0704-0188

1. AGENCY USE ONLY (Leave blank)	2. REPORT DATE 6 July 1995	3. REPORT TYPE AND DATES COVERED Final Report

4. TITLE AND SUBTITLE

Mid Infrared Diode Lasers Based on III-V Alloys for the Spectral Range 3-3.5 μm Operating Near Room Temperature

5. FUNDING NUMBERS

F6170894C0011

6. AUTHOR(S)

Dr. Yury Yakovlev

7. PERFORMING ORGANIZATION NAME(S) AND ADDRESS(ES)

SEC for Microelectronics of Ioffe Physico-Technical Institute
26 Polytechnicheskaya St
St. Petersburg 194021
Russia

8. PERFORMING ORGANIZATION REPORT NUMBER

N/A

9. SPONSORING/MONITORING AGENCY NAME(S) AND ADDRESS(ES)

EOARD
PSC 802 BOX 14
FPO 09499-0200

10. SPONSORING/MONITORING AGENCY REPORT NUMBER

SPC 94-4047

11. SUPPLEMENTARY NOTES

12a. DISTRIBUTION/AVAILABILITY STATEMENT

Approved for public release; distribution is unlimited.

12b. DISTRIBUTION CODE

A

13. ABSTRACT (Maximum 200 words)

This report results from a contract tasking SEC for Microelectronics of Ioffe Physico-Technical Institute as follows: Design and produce Mid IR (3-3.5 micron wavelength) diode lasers, capable of operating near room temperatures, using the III-V alloys InAsSbP and InAsSb.

14. SUBJECT TERMS

EOARD

15. NUMBER OF PAGES

48

16. PRICE CODE

N/A

17. SECURITY CLASSIFICATION OF REPORT	18. SECURITY CLASSIFICATION OF THIS PAGE	19. SECURITY CLASSIFICATION OF ABSTRACT	20. LIMITATION OF ABSTRACT
UNCLASSIFIED	UNCLASSIFIED	UNCLASSIFIED	UL

NSN 7540-01-280-5500

Standard Form 298 (Rev. 2-89)
Prescribed by ANSI Std. 239-18
298-102

PROJECT MANAGER:

Yuri P. Yakovlev, Dr. Sci
head of infrared optoelectronics laboratory

KEY PERSONS

Maya P. Mikhailova, Deputy project manager, Dr. Sci., l.r.s.
Albert N. Imenkov, Dr. Sci., l.r.s.
Georgy G. Zegrya, Ph. D., s.r.s.

INVESTIGATORS

Tamara N. Danilova, Ph. D., r.s.
Oleg G. Ershov, j.r.s.
Konstantin D. Moiseyev, Ph. D., j.r.s.
Alexander M. Litvak, Ph. D., s.r.s.
Andrei A. Popov, Ph. D., r.s.
Victor A. Solov'ev, Ph. D., s.r.s.
Alexey D. Andreyev, j.r.s.
Semen G. Konnikov, Dr. Sci., l.r.s.

- *lead research scientist—l.r.s.*
- *senior research scientist—s.r.s.*
- *research scientist—r.s.*
- *junior research scientist—j.r.s.*

CONTENT:

ABSTRACT

This work is devoted to creation and investigation of mid infrared lasers based on InAsSb/InAsSbP for the spectral range 3-3.5 μm operating near room temperature. Epitaxial technology of double heterostructure lasers and separate optical and electron confinement (SOEC) laser structures was developed. Quaternary InAsSbP layers with high phosphorous content (31-35%) were grown to improve confinement layers.

Main characteristics of the laser structures were investigated. Threshold current dependence was studied both theoretically and experimentally including strained structures.

High operating temperature T=203 K was achieved in pulse regime for InAsSb/InAsSbP SEOC lasers. It was predicted on the base of the theoretical analysis that lasing can be achieved up to 250 K. Further increasing operation temperature (more than 250K) is mainly limited by rising non-radiative recombination losses as it is confirmed by experimental and theoretical data. It leads to necessity for search new non-traditional ways to laser design.

In the frame of this work we proposed new physical approach to middle infrared lasers with higher operating temperature creation. Novel tunnel-injection laser based on type II broken-gap isotype p-p single heterojunction was realized. Intensive spontaneous and coherent emission was achieved in multi-layers laser structure with p-GaInAsSb/p-InAs(InGaAsSb) heterojunction in active layer. Effect under study is due to indirect (tunnel) radiative recombination of spatially separated electrons and holes localized in quantum wells at different sides of the heteroboundary. Suppression of non-radiative Auger recombination rate on type II heteroboundary was theoretically predicted and experimentally observed.

High characteristic temperature T_0=40-60 K was achieved in the range of 77-120 K in novel laser structures.

Main results obtained in the frame of the project open the way to increase operation temperature of middle infrared diode lasers up to room temperature.

INTRODUCTION

During several last years a great interest have been increasing in creating and studying of MID infrared diode lasers for the spectral range 2-5 μm. There are many important applications of such devises including optical communications on the base of fluoride glass, eye-safe laser radars, remote sensing of atmospheric gases, some medical applications, precise control for high technology in industry and so on. The molecular vibration bands and overtones of various substances are in the spectral range 2-5 μm and they can be identified with high accuracy by means of tunable diode laser spectroscopy. (TDLS) [1].

Now there are more than 130 research groups in 17 countries which deal with TDLS studying, 20 of them are in the former Soviet Union [1]. MID IR range TDLS technology exists in USA, Russia, Canada, China, Germany.

At present all developed countries carry out the program of the atmosphere impuring to solve the global geophysical problems. The problem is discussed on the TDLS application for the planet atmosphere monitoring during the automatic interplanetary station's space flights.

High TDLs sensitivity for the resonance absorption registering (10^{-4}-10^{-5} of the integral power), high frequency scanning and total selectivity of the analysis of the multicomponent gas mixtures provides the possibility of solving different problems for gas analysis and diagnostics by TDLS methods. Further sensitivity increasing is limited by the properties of IR lasers [2].

However, up today there are only several scientific centres (about ten), concerning with growing, research and designing MID IR lasers based on III-V alloys (2-4 μm) [3-5] and II-IV alloys (lead salts, 3-30 μm) [6].

Recently a great attention have been paid to IR lasers based on GaInAsSb solid solutions operating at room temperature. But there are a big region of immiscibility in the range of the composition x>0.25 and it doesn't allow to get lasers with the emission wavelength more than 2.5 μm [7].

The "black spot" between the GaInAsSb lasers and lead salt lasers can be covered by laser based on InAs solid solutions such as InAs and InAsSbP (2.7-4 μm) [8].

Only a few groups deals with III-V MID IR lasers for this spectral range based on InAs alloys. Main of them MIT Lincoln Lab., David Sarnoff Research Centre, Hughes Lab., AT&T Bell Lab. , Sandia National Lab. in the USA, Centre of Microoptoelectronic, Montpellier II, France, Nippon Telephone and Telegraph Corp., Japan, and Ioffe Physical Technical Institute, St.Petersburg, Russia.

MID IR lasers based on InAsSbP/InAs or InAsSbP/InAsSb heterojunctions have been grown by LPE [8,9], MOCVD [10] or MBE methods [11] and can only operate in pulse and cw regime at low temperatures (up to date pulse operation was achieved in the range of 77-180 K, CW operation up to 78-100 K).

There are several fundamental physical limitations which obstructs to further increasing operating temperature of the narrow-gap lasers and obtaining coherent generation up to room temperatures.

First of all there is a problem of non–radiative Auger recombination which contribution is especially large in narrow-gap semiconductor materials based on InAs alloys with near–resonance band structure ($E_g=\Delta_0$, energy gap is equal to spin-orbit splitting value of the valence band) [12,13]. Then, electron heating can play a significant role in InAs and other narrow gap semiconductors at low temperatures [14]. Third, there is a problem of improving electron and optical confinement which can be solved for lasers based on InAsSb by growing InAsSbP confinement layers with higher P content (more than 30%) taking into account small difference of refractive indices of InAs and InAsSbP. For example, for P content 10-18% in confinement layers as it was established in [9] this difference was about 0.01-0.02. It is not sufficient to get good optical confinement and to increase operating temperature of MID IR lasers.

The increasing operating temperature with decreasing threshold current density and leakage currents can be achieved as a first step using laser structures with improved electron and optical confinement, and then, using novel types of lasers with strain active layers or quantum well structures and/or new types of heterostructures.

Recently in [11,16] it was shown that significant decreasing threshold currents and increasing cw output optical power was achieved in long-wavelength GaInAsSb/GaAlAsSb lasers (2.1-2.3 μm) by using of strained structure multi-quantum wells in the active region and very good confinement layers with high Al content. Characteristic temperature in such structures was found T_0=113 K in the range 20-50^0 C and T_0=45 K in the range 100-150^0 C which demonstrates a great possibility of broadening operating temperature range of longwavelength lasers.

Up to beginning this work the highest operating temperature which was achieved for MID IR lasers based on III-V quaternary alloys was about 160-180 K in pulse regime and characteristic temperature T_0=26-30K [17].

PROGRAM OBJECTIVE

The main goal of this proposal is to increase operating temperature of MID IR lasers based on III-V InAsSb/InAsSbP alloys up to near room temperature.
This work was proposed as two-years program.
During first year **we were going to solve the following basic tasks**:

1. To carry out theoretical and experimental studying thermodynamic phase equilibrium and immiscibility gap in InAsSbP solid solutions lattice-matched with InAs substrata to get wide-gap confinement layers with high P content.

2. To grow multilayer laser structure based on InAs/InAsSb/InAsSbP alloys with improved electron and optical confinement and to investigate temperature dependence of main characteristics of the diode laser structures both based on double heterostructures and multilayer structures with separate optical and electron confinement.

3. To study fundamental physical causes limiting high-temperature operation of MID IR lasers, first of all non-radiative Auger recombination processes.

4. To propose new physical approaches to design of mid-infrared lasers operating at high temperatures.

TECHNICAL SCHEDULE

I Phase (1st year) July 1, 1994 / June 30, 1995

The creation and studying of the lasers based on InAsSbP/InAsSb for the spectral range 3.0-3.5 μm with improved optical and electron confinements.

1. Creation of mid-IR laser diodes

1a. The theoretical and experimental studying phase-equilibrium and miscibility gap of multicompcnent solid solutions InAsSbP lattice-matched with InAs substrate.

lb. LPE growing InAsSbP alloys with the highest P content. LPE growing InAsSb/InAs thin active layers.

lc. X-ray diagnostic, photoluminescence, electroluminiscence and physical-chemical studying laser heterostructures.

1d. LPE growing laser structures with thin active layers and improved confinement layers.

2. Creation and study of mesa stripe lasers with improved confinement

2a,b. Fabrication of laser diodes. Investigation of spontaneous and coherent luminescence and quantum efficiency of the lasers with improved confinement in the temperature range 77-250 K.

2c. Theoretical calculation and experimental studying of the temperature dependence of the threshold current density in laser structure with improved confinement and different resonator lengths.

2d. Theoretical and experimental studying of physical causes limiting operation of mid-IR lasers at high temperatures.

3. Creation and studying MID IR lasers with strain active layers and improved confinement based on InAsSb/InAsSbP

3a. LPE- growing laser structures with strain active layers.

3b. X-ray diagnostics, physical-chemical and photoluminescence, electroluminescence investigations of layers and heterostructures

3c. Fabricating mesa stripe laser diodes and broad area lasers on the base of strain structures

3d. Theoretical studying of radiative and non-radiative Auger recombination in the narrow-gap structures

4. Comparing studying of mid-infrared laser diodes characteristics with unstrained and strained active layers depending on temperature

4a. Analysis and comparing of nonradiative Auger processes in laser structures with unstrained and strained layers

4b. Analysis of leakage currents in strain laser structures.

4c. Investigation of the strain influence on limit operating temperature of InAsSbP/InAsSb diodes.

I. The creation and studying of the lasers based on InAsSbP/InAsSb for the spectral range 3.0-3.5μm with improved optical and electron confinements

1. Creation of mid IR laser diodes

Ia. The theoretical and experimental studying phase-equilibrium and miscibility gap of multicomponent InAsSbP solid solutions lattice-matched with InAs substrate

LPE growing multicomponent InAsSbP alloys with high phosphorous content requires an application of mathematical methods for calculation of liquidus-solidus phase diagrams and determination of the composition of liquid phase. For this purpose we use new more accuracy thermodynamic method in comparing with traditional models which were not suitable for accurate calculation such complicate system as quaternary solution In-As-Sb-P (InAs-InSb-InP) in wide temperature, concentration and composition range.

Our theoretical method based on excess thermodynamic linear functions-combinations of standard chemical potentials was developed in [18] and was before applicated to calculate the miscibility region of solid system Ga-In-As-Sb layer-GaSb substrate [19, 20].
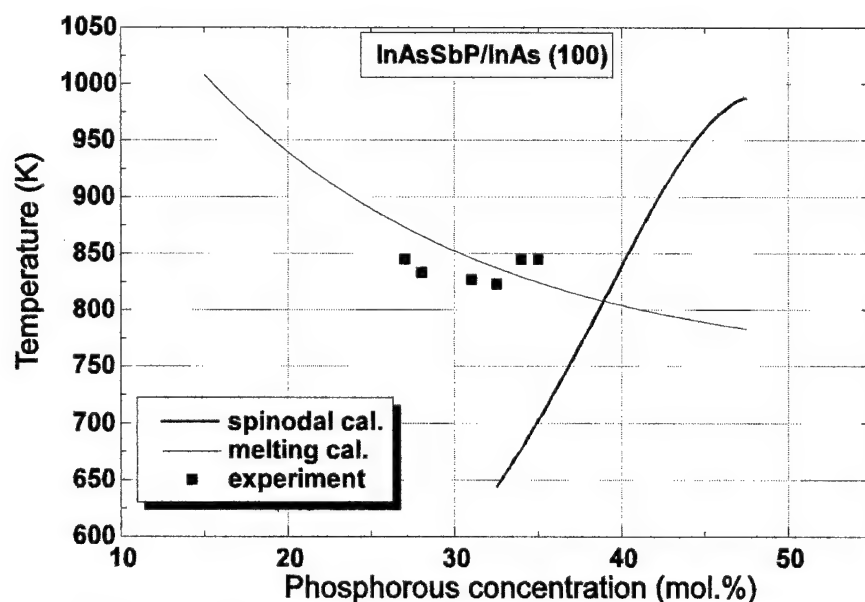

Fig. 1. The miscibility region of InAsSbP layers lattice-matched to InAs(100) calculated theoretically and obtained experimentally by LPE

In the frame of the project we calculate isotherms of liquidus and solidus of quaternary system In-As-Sb-P using developed theoretical model and found a

region of existence of the these solid solutions [20]. The calculation shows that higher growth temperatures are necessary to obtain phosphorous-rich alloys with wider-band gap for confined layers.

Fig.1 represents so-called spinodal curve where the maxima of solid composition x (InP) lattice-matched with InAs substrate are plotted as a function of temperature. Points represents our experimental results. There are two regions in Fig. 1. The first one is the region of the spinodal decomposition and it has a fundamental physical origin, and the second one connects with the conditions of LPE growing (melt temperature of multicomponent solid solutions).

1b. LPE growing InAsSbP alloys with the highest P content. LPE growing InAsSb/InAs thin active layers with critical thickness.
1c. X-ray diagnostics, PL, EL and physico-chemical studying laser heterostructures.

Quantative electron probe microanalysis (EPMA) of InAsSbP/InAs, InAsSb/InAs and InAsSbP/GaSb heterostructures was made by using X-ray microanalyser CAMEBAX Microbeam (Cameca). Experiment conditions were optimise for sensitivity, accuracy, representation locality. Quantitive analysis was carried out by lines of InL_α, AsL_α, SbL_α, PK_α. Measuring of X-ray intensity was made in differential regime to exclude overlapping AsL_α line under study and third order line SbL_α. As an exterior ethalon we used binaries InAs, InP, GaSb.

Detectivity limit was in the range of 0.5-1 % depending on element under study. Locality of the analysis during measure of solid solution composition in the systems In-As-Sb-P and In-As-Sb was L =0.5-0.8 μm, L =1.5-3 μm depending on analysed element. The error is so-much 2.0 % for In, 3 % for Sb and 3.0 % for P. Fig.2 represents typical distribution of In, As, Sb, P elements at cleavage of InAs/InAsSbP heterostructure.

Taking into account results of points 1a and 1b we can fabricate InAsSbP epitaxial layers by LPE method with high InP content up to 40 mole percentages at T=820 K (547^0C). However, we used in our work LPE grown temperature about 843-873 K ($570-600^0$C), which was more convenient for growing all layers of DH laser structure based on InAs alloy including active and confinement layers in the whole technological cycle.

So, we made laser structures with confined layers with maximum P content of 31-35%. In this case band gap difference between InAsSb active layer (x= 0.04 - 0.06, Eg = 0.414-0.354 eV) and InAsSbP confined layers was ΔE_g=147-170 meV
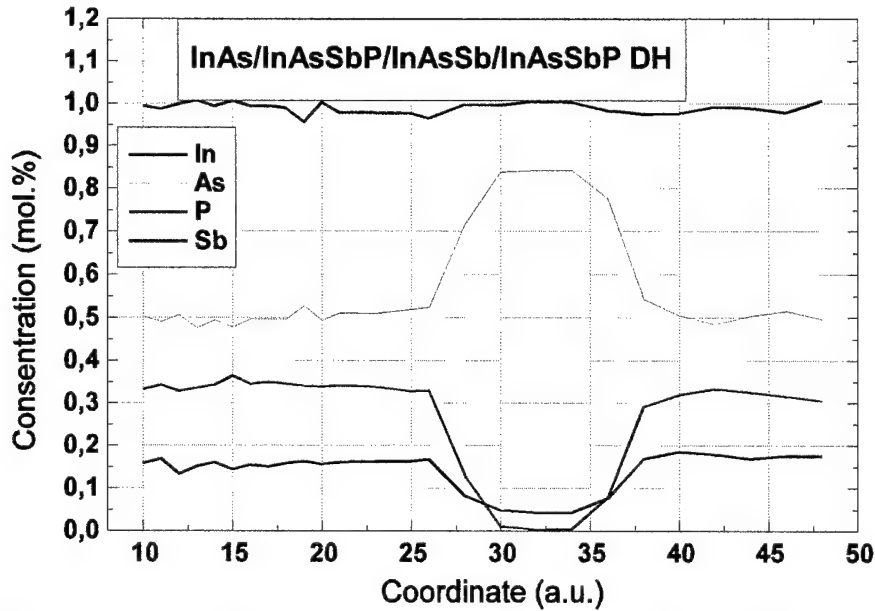
Fig.2. Cleaved facet distributions of elements in the alloys in the DH with high Phosphorous content claddings which was measured by X-ray microprobe analyser.

which was sufficient for electron and optical confinement.

In our experiments InAsSbP layers with P content from 12 up to 35 % were grown and studied and a composition of InAsSbP alloys and lattice-matching were determined. Lattice-matched InAsSbP layers with InAs was $\Delta a/a < 2 \times 10^{-4}$. A composition of InAsSbP alloy was found from X-ray diagnostic.

Energy band gap of InAsSbP alloys was established from photoluminescence measurements at T=77K (See Fig. 3). Theoretical calculation of energy band gap was carried out by using approximate formula [21]:

$$E_g = E_g (InAs)(1-x-y) + E_g(InP)x + E_g(InSb)y + xyC(InSbP) + \\ + x(1-x-y) C(InAsP) + +y(1-y-x) C(InAsSb), \qquad (1)$$

where C are the bowing parameters. Good agreement was achievement in our case between calculation and PL experiment as it can see from Fig.3.

Galvanomagnetic properties of quaternary InAsSbP were also studied. Hall electron mobility was measured in Te doped n-InAsSbP layers (x=0.26-0.31) grown on semi-isolating p-InAs substrate. Hall electron mobility was determined in the range of u_H = 10,000-13,000 cm^2/Vs. Energy gap value E_g of InAsSbP layer with P = 26% was studied in dependence on doping level also by photoconductivity spectra. It was found blue shift of E_g value with doping increase from 10^{16} up to 5×10^{18} cm^{-3} due to Burstein-Moss effect.
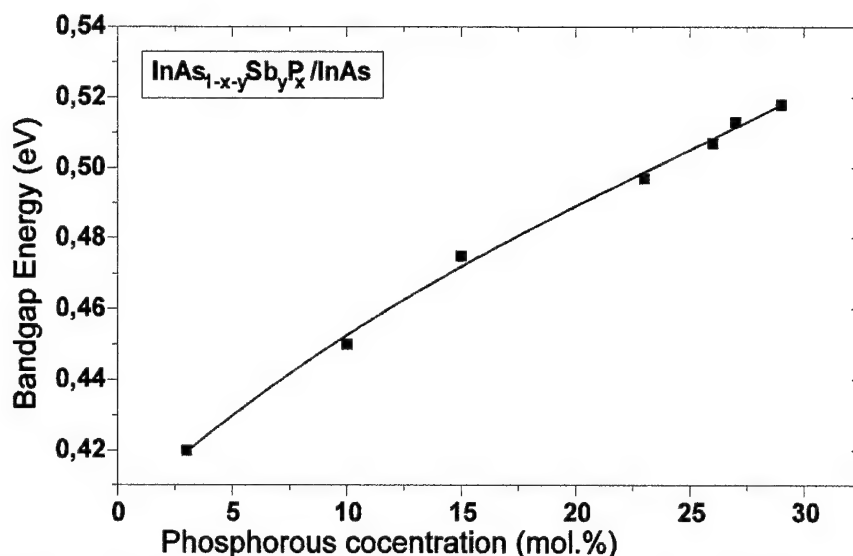
Fig.3. Energy bandgap of the InAsSbP layers lattice-matched to InAs(100) determined by photoluminescence method at LN_2 temperature as function of phosphorous concentration

1d. LPE growing laser structures with thin active layers and improved confinement layers

Laser structure were grown by LPE on InAs(100) substrata with hole concentration $p = 2*10^{18}$ cm^{-3} at T=570-600^{0}C. Cladding layers of P-InAsSb$_{0.26}$ were doped by Zn up to $p = 2*10^{18}$ cm^{-3} and their thickness was d=2.5 μm. Undoped active layers of InAsSb (x=0.04-0.06) and quaternary InGaAsSbP were grown with p= $5*10^{16}$ cm^{-3}. Their composition and lattice-matching were also determined by X-ray diagnostic.

Energy band gap of active layers was in the range E$_g$=0.414-0.354 eV and corresponds to emission range of 3-3.5 μm. Thickness of active layers was in the range of d = 0.3 - 1.5 μm. Thinner layers (d =0.1-0.3 μm) were slightly strained. Confined layers of n-type InAsSbP (InP is 31-35%) were doped by Sn up to p = 5 x10^{17} cm^{-3} and had a thickness of 2 μm. Ohmic contacts were made from Au: Ge (p-layers) and Au: Te (n-layers) alloys by vacuum deposition and by fusion in H$_2$ atmosphere at T = 400 C.

Electroluminescence was measured to control a quality of DH InAs/InAsSbP/InAsSb/InAsSbP laser structures. Fig. 4 represents spontaneous emission spectra one of the typical laser structures at T =77K and 300 K.

In the frame of this work unique method was developed for analysis of the narrow-gap semiconductor homo- and heterostructures by scanning electron microscopy. It was described in [22].

In the case of multilayer heterostructures the precise measurement of p-n junction position relatively the specific heterointerface becomes very important. For p-n junction location measurements of electron beam induced current (EBIC) mode
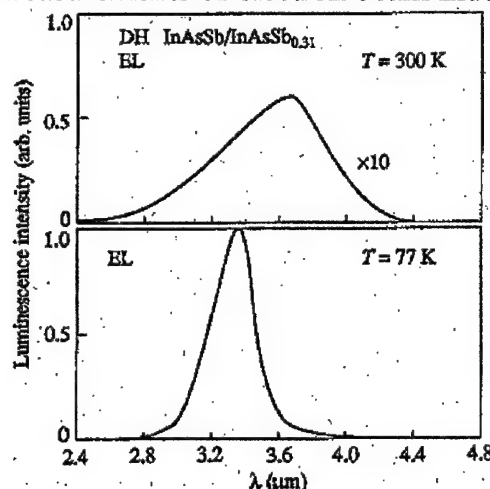

Figure 4. Electroluminescence of DH InAsSb/InAsSbP laser structure at T = 300 K and 77 K.

in a scanning electron microscope (SEM) was used. Our investigations shown that the identification and precise measurement of position of the interfaces at InAs-based heterostructures is not trivial.

We have studied the specific features of signal formation in secondary electron (SE) and backscattering electron (BSE) modes. These modes are mostly used in SEM for characterisation of layers with different chemical composition. Two types of structures were investigated:

I. Structures based on the quaternary solid solutions GaInAsSb with composition near to InAs and GaSb respectively.

The feature of such structures is that the average atomic numbers of compounds are very closed (the average atomic numbers of InAs and GaSb are equal). Therefore the contrast in BSE mode which is proportional to average atomic number difference of the components must be disappeared. However, weak contrast in SE mode as well as in BSE mode were experimentally observed (Fig. 6).

We found out that:

1) SE contrast is not stable. There is SE contrast which is opposite to BSE contrast if only single scanning of cleaved plane region not radiated is used. In the case of multiple scanning it is decreased and become similar to the BSE contrast.

2) There is a contrast in SE mode named voltage contrast which is due to p-n junction presence in the structure. It can be used for p-n junction position measurement but only in the case when the distance between p-n junction and heterointerface is more than 0.3 - 0.5 μm.

3) BSE coefficient for compounds with composition near to InAs is more than one for compounds with composition near to GaSb. When the electron beam scans across an abrupt interface BSE contrast does not change monotonous but shows a "dip" and a "bump". This effect we investigated early
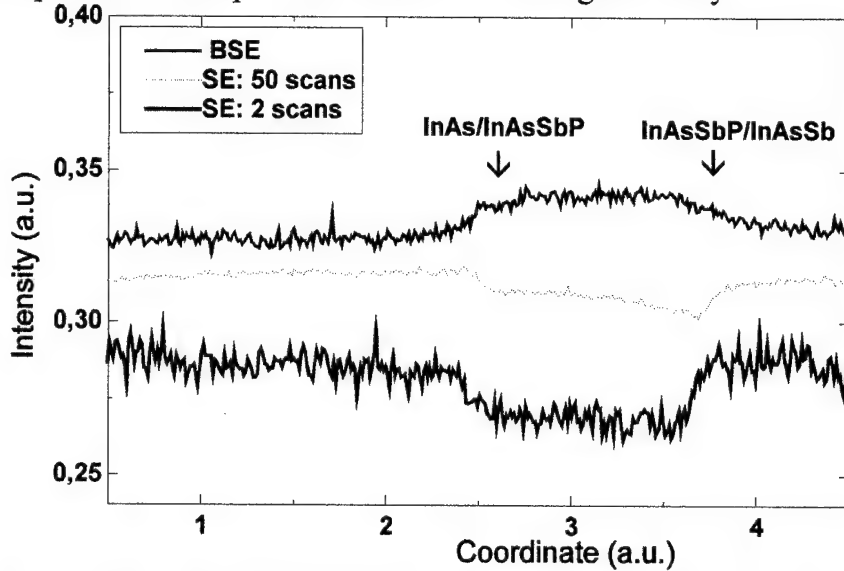
Fig.6. Contract in BSE (backscattering electrons) and SE (secondary electrons) signals under SEM measurements on the cleaved facet of the heterostructure

Fig.7. Signal contract in BSE and SE modes which was used for SEM measurements of the positions p/n junction relative to the interface

in AlGaAs-GaAs structures and due to the atomic-number dependence of the electron scattering in a finite size interaction volume where the average atomic number is spatially non-uniform. The co-ordinate of BSE signal derivative

maximum corresponds to the position of interface. Interface BSE contrast does not change monotone but shows a "dip" and a "bump".

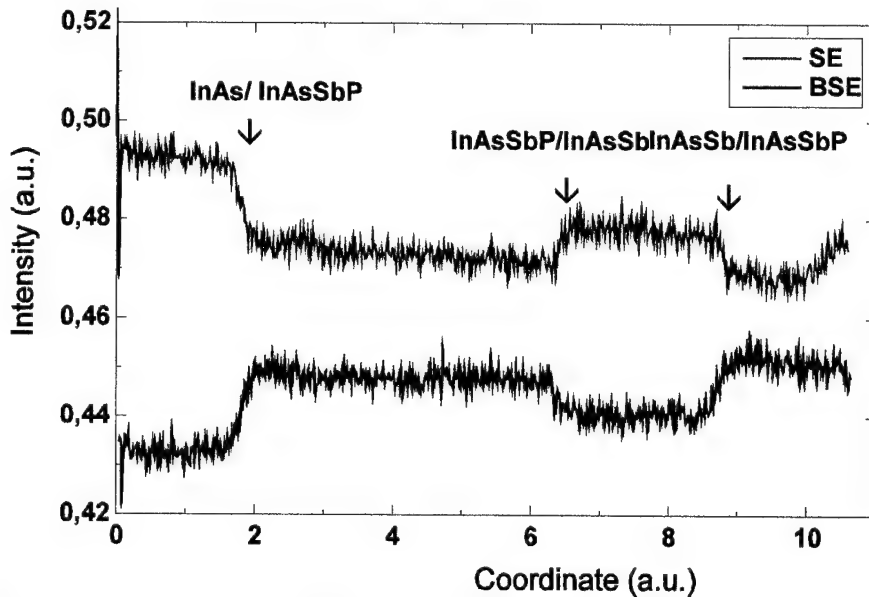4) Comparative analysis of BSE and SE contrast line profiles obtained on the crystallographically cleaved plane show that BSE mode is more preferable for correct measurements of InAs-based heterointerface position. It is more stable, it has better signal/noise ratio and it is increased at heterojunction more sharp.

II. Structures based on the quaternary solid solutions InAsSbP.

We have studied the structures contained InAs, InAsSb, InAsSbP (0.1 and 0.3 mole part of phosphorous). The difference of the average atomic numbers for such compounds is very small and BSE contrast is very weak so (in compare with AlGaAs-GaAs system ,for example). Therefore, to except artefacts and to measure interface position more precisely the surface of sample cleaved plane studied must be crystallographic and near to ideal one.

Our investigations showed that:

1) BSE contrast under single scanning of electron beam through the cleaved plane not radiated initially.
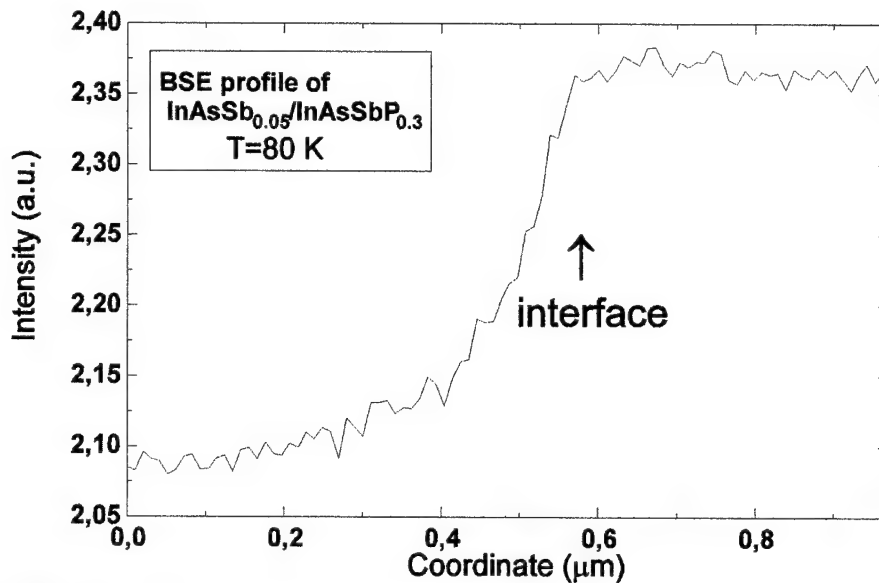
Fig.8. BSE profile measured across graded InAsSb/InAsSbP interface

2) BSE coefficient for InAsSbP compounds under study is more than one for InAs and InAsSb. But BSE contrast line profiles obtained in studies of abrupt heterojunction InAsSbP-InAs (Fig.8) and InAsSbP-InAsSb differ radically from ones obtained for AlGaAs-GaAs and have a typical zig-zag form (Fig.9). The region of sharp rising of BSE signal corresponds to moving of electron beam (which have Gaussian distribution and is of 30-40 nm in diameter) across the interface. The smoother is the heterojunction studied, the smaller is the jump in

BSE profile. In structures with graded interface this feature is disappeared at all and the BSE profile

Fig.9. BSE profile measured across abrupt InAsSb/InAsSbP interface

become monotone. Fig.8 show the BSE line profile obtained at InAsSb - gradient InAsSbP interface. Therefore, the possibility of heterointerface sharpness identification is a powerful feature of BSE mode which we using for analysis p-n junctions in our laser structures.

II. Creation and studying of mesa-stripe lasers with improved confinement.

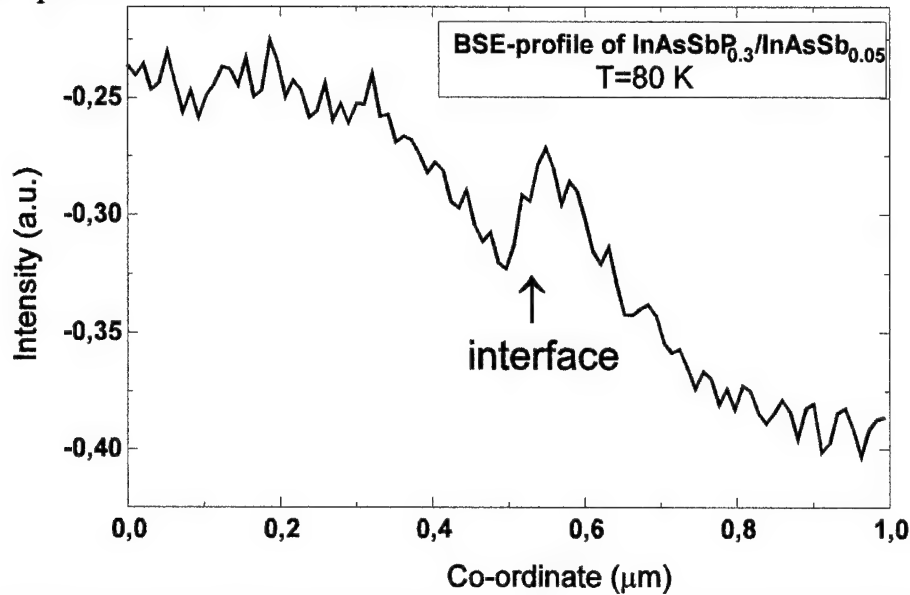## 2.a.b. Fabrication of laser diodes. Investigation of spontaneous and coherent luminescence and quantum efficiency of the lasers with improved confinement in the temperature range 77-250K.

InAsSb/InAsSbP double heterostructure lasers were fabricated as it was described briefly in Section 1. Here we represent some results of spontaneous and coherent luminescence and quantum efficiency studying for type-I DH lasers as well as threshold current dependence on active and confinement layer thickness and cavity length.

Mesa stripe lasers were made by strip width of 12-55 μm. Fig.10 represents threshold current dependence on cavity length. Threshold current
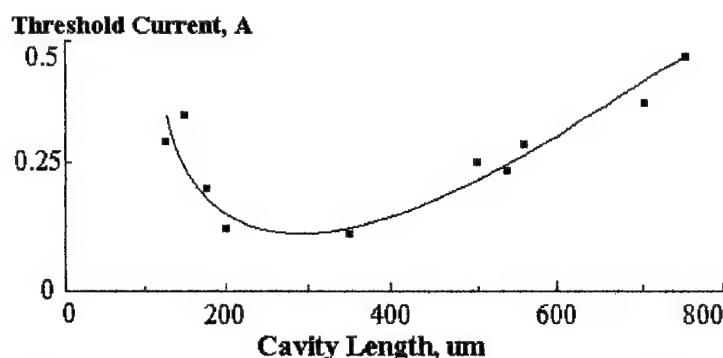
Fig.10. Threshold current versus cavity length in InAsSb/InAsSbP DH lasers.

was measured in pulse regime with pulse duration 100 ns and repetition frequency 5 kHz. We established that optimum value of cavity length was in the range of 250-300 μm. Optimum thickness of active layer was 0.5-1 μm. Spontaneous and coherent emission spectra versus drive current were studied. As one can see from Fig.11 coherent emission arises in the centre of the maximum spontaneous band.

Single-mode generation with TM-polarisation of radiation predominanced in our lasers under study. Fig.12 and Fig.13 represent temperature dependence of InAsSbP/InAsSb DH lasers with P content of 19% and 35%, respectively. In the first case we can obtain operating temperature 140-150K only, but in the second case operating temperature up to 178-185 K was achieved.

Threshold currents value depended also from thickness of confinement layer as it is shown in Fig.13. The lowest threshold current was obtained with thinner InAsSbP confined layer of 1.5 μm thickness.

Temperature dependence of threshold current was described by exponential equation $I_{th}=I_0 exp(T/T_0)$, where characteristic temperature T_0 was obtained
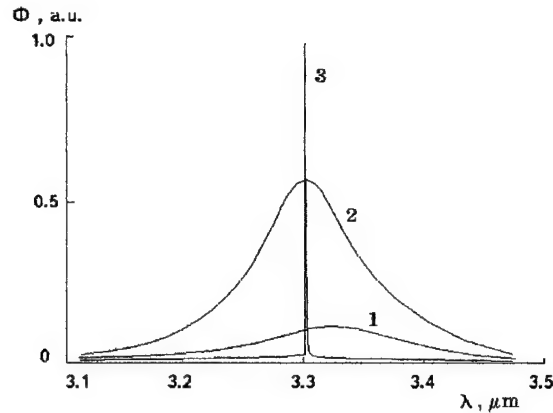
Fig.11. Spectra of spontaneous and coherent emission of InAsSb/InAsSbP DH laser at drive current, mA: 1-30, 2-90, 3-95.
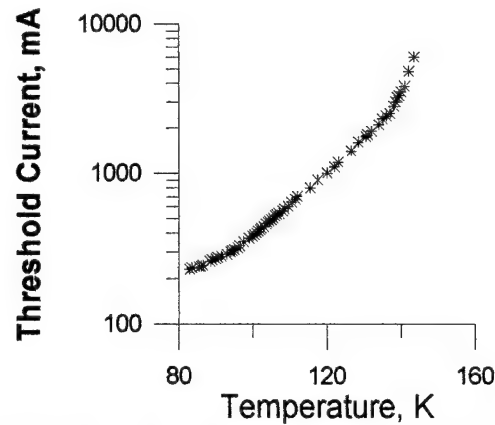
Fig.12. Temperature dependence of threshold current of InAsSb/InAsSbP laser. Confined layers of InAsSbP with P content of 19%.
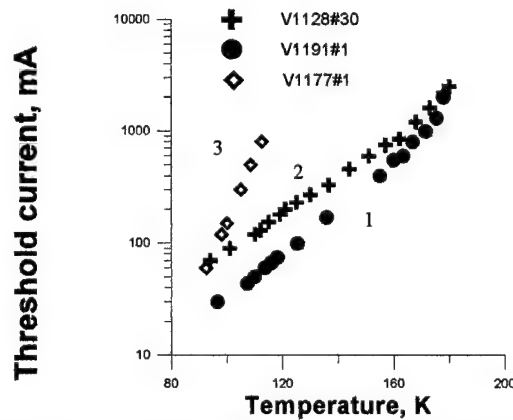
Fig.13. Temperature dependencies of threshold current of InAsSb/InAsSbP DH laser with higher P content of 35% in confinement layers of various thickness d, μm: 1--3, 2-2.8, 3-1.5.
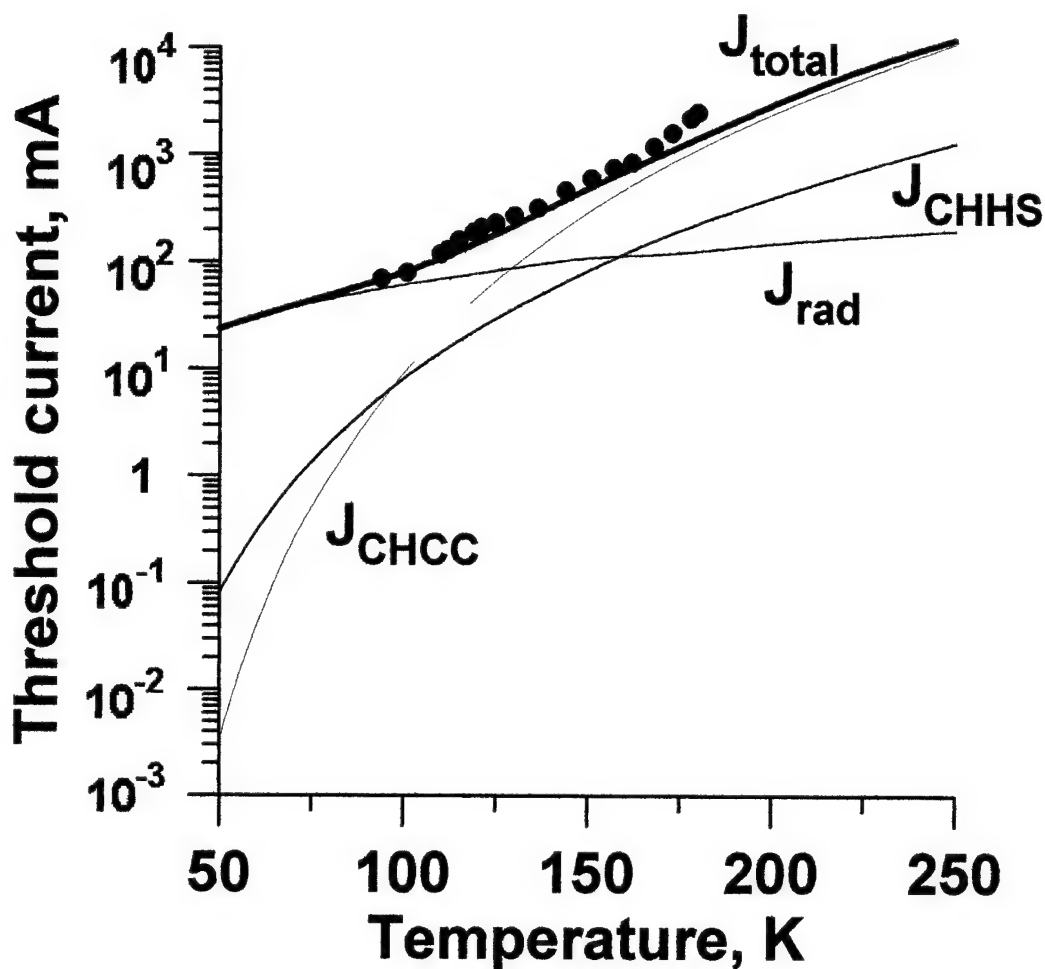
Fig.14. Theoretical temperature dependence of threshold current density of InAsSb/InAsSbP DH lasers calculated with taken into account various recombination processes:

----- - radiative process; _._. and - - - non-radiative Auger-processes CHHS and CCHC, respectively, solid curve- total threshold current, dark squares are experimental data for InAsSb/InAsSbP DH laser with high P content of 35%.

T_0=19-20K for lasers with lower P content confined layer, and T_0=25-30K for laser structures with improved confined layers.

2.c. Theoretical calculation and experimental studying temperature dependence of the threshold current density in laser structure with improved confinement and different resonator lengths.

2.c.1. Theoretical calculation of threshold current temperature dependence

Here we consider main factors which influence threshold current temperature dependence of InAsSb/InAsSbP heterolasers.

It is known that threshold current I_{th} in III-V longwavelength lasers is determined by four main recombination processes:

i) radiative recombination process with temperature dependence $I_{th} \sim T^{3/2}$ and by three non-radiative Auger-recombination processes;

ii) CHHS-process, in which energy of recombine electron-hole pair passes to hole in spin-orbit splitting valence band. Temperature dependence of this process is $I_{thCHHS} \sim T^{9/2}$ [24,25], and it is very effective in materials with $E_g > \Delta_o$, where Δ_0 is a value of spin-orbit splitting of the valence band [26];

iii) non-radiative CHCC-process in which energy of recombine carriers passed to high-energy electron in the conduction band. This process has a temperature dependence as $I_{th}^{CHCC} \sim T^4 exp(-E_{th}/T)$ [25];

iiii) novel threshold-less Auger recombination process due to electron interaction with a heteroboundary with temperature dependence of the threshold current $I_{thA} \sim T^{11/2}$ [26].

Results of the theoretical calculation of threshold current due to above mention processes are represented in Fig.14 by dashed curves. Total threshold current is shown by solid curve. Dark squares are our experimental data for InAsSb/InAsSbP DH laser with improved confinement with P content 31-35% which parameters are represented in points 2a,b.

From theoretical analysis we can conclude that only three recombination processes contribute in the threshold current value: radiative recombination and non-radiative CHHS- and CCHC-processes. At higher temperature T>100K CCHC process prevails over others. But at low temperatures (T<100K) only radiative recombination process contributes threshold current. For decreasing threshold current and increasing internal quantum efficiency of the lasers which can be represented as:

$$\eta_{int} = \tau_r/(\tau_r + \tau_A) = I_{th}/(I_{thR} + I_{thA}) \qquad (2)$$

where I_{thR} and I_{thA} are current components determined by radiative and non–radiative recombination processes, non-radiative Auger-process must be suppressed. Some methods of suppression of non-radiative Auger-recombination will be discussed in Section IV. It can be fulfilled by increase of difference Δ_o-E_g, which will lead to decreasing CHHS-Auger process.

In our experiment we observed that cavity length influence slightly threshold current (Fig.10). But barrier height of the confined layers plays an important role. In the same temperature range where Auger-recombination dominanced energy E_A of excited Auger-electrons and holes are always higher than barrier heights ΔE_c and ΔE_v, (E_A~E_g of the narrow-gap active layer). Hence for improving electron confinement it is need ΔE_c and ΔE_v being in order to E_g of narrow-gap layers. With using InAsSbP confined layers with higher P content (31-35%) we succeeded in decreasing twofold threshold current of our lasers comparing with laser structures with 19% of P content in confined layers (see Fig.12 and 13) and we succeeded in increase of operating temperature in pulse regime from 140-150 up to 180K. As it is seen from Fig.14, at higher temperatures non-radiative Auger-processes dominanced in the threshold current value and it leads to more sharp increase of threshold current at T>180K.

We can conclude that experimental threshold current density of our InAsSb/InAsSbP DH lasers is good described by theoretical curves taking into account all main channels of the radiative and non-radiative Auger recombination.

2.C.2. Experimental studying. Discussion on temperature dependence of laser performance

Multilayer (3 or 5-layers) laser structures were fabricated by LPE on InAs (100) substrate. Double heterostructure (3-layers) or structure with separate electron and optical confinement (SEOC) (5-layers) were made (Fig.15). Energy band gaps of InAsSb active layer and InAsSbP confined layers were in the range of E_g= 0.320-0.410 eV and E_g=0.547-0.602 eV, respectively at T=77K. Energy band diagram of DH InAsSb/InAsSbP was a type I with band offsets ΔE_c=144 meV, ΔE_v=28 meV , SEOC laser structures with additional InAs layer in an active layer were nearly to type II with small values of band offsets (ΔE_c=15 meV and ΔE_v=54 meV) at 77K. Calculated difference of refractive indices between active and confined layers was Δn=0.04-0.07. Thickness of active layers were d=0.6-1.5 μm, and emitter layers d=2-3 μm. Mesa-stripe lasers were made with stripe width 12-55 μm, and cavity length from 200 to 2000 μm.
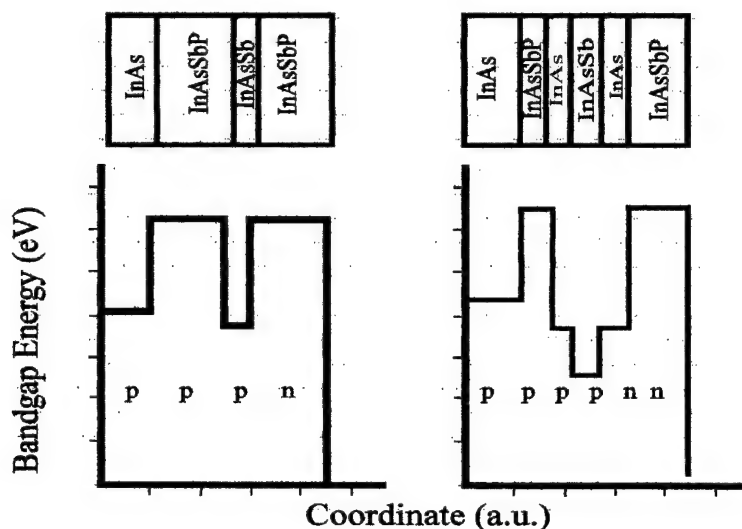
Fig.15. The bandgap energy diagrams of the heterostructures that were fabricated.

Pulse regime operation of these lasers was studied with pulse duration 100 ns and repetition frequency 10^5 Hz.

Typical coherent spectra one of the DH laser under study are represented in Fig.16 for various temperatures. This laser structure has InAsSb active layer with E_g=0.375 eV ($\lambda \cong 3.37$ μm) and InAsSbP confined layers E_g=0.547 eV. Cavity length is ~ 300 μm, thickness of active and emitter layers is 0.6 μm, 2.3 μm and 2.7 μm respectively. Stripe width was 45 μm.

Lasing spectrum is single-mode at current value I~1.2I_{th}, and it is valid up to T~160K.
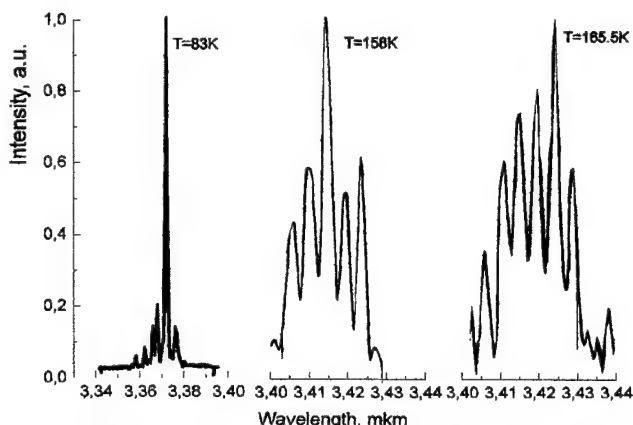
Fig. 16. Spectra of InAsSb/InAsSbP DH laser (diode #V1126-80) at three temperatures: a - T=83K, I = 2I_{th}; b - T=150K, I = 2I_{th}; c - T=165,5K, I = 2I_{th}.

Intensity-current characteristic (see Fig.17) at small current values (spontaneous mode) has small inclination. After reaching threshold of inversion I_i the curve under study is sloping upwards smoothly with current
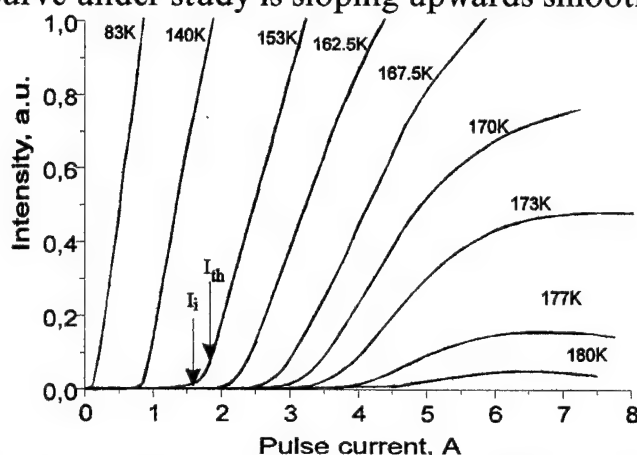
Fig. 17. Intensity-current characteristic for InAsSb/InAsSbP DH at various temperatures. I_i - inversion threshold current, I_{th} - threshold current at coherent generation (diode #1126-80).

rising. And then , after achievement of threshold current of generation I_{th}, the intensity-current characteristic is practically linear at current values above 1-3 times threshold current and temperature lower than 160K. At further temperature increasing a linear part of the characteristic changes on sublinear one and length of the linear part scales down. The linear part of the characteristic is absent at T >170 K.

Temperature dependence of I_{th} and I_i deduced from intensity-current dependencies at various temperatures represents in Fig.18. As one can see
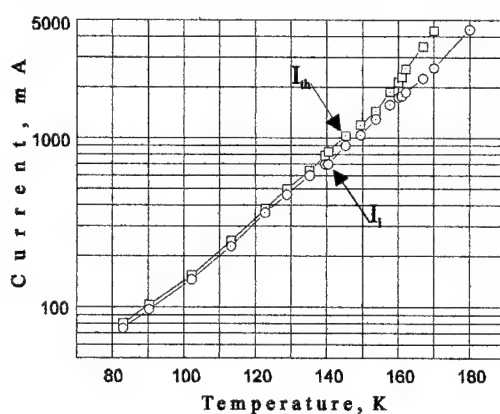
Fig. 18. Temperature dependence of inversion threshold current I_i and threshold current I_{th} of DH laser structure InAsSb/InAsSbP (diode #1126-80).

As a result in order to improve the parameters of the mid- infrared double-heterostructure lasers operating at high temperatures it is necessary to optimise a laser structure in which the non-radiative processes listed above will be weakened. Theoretical analysis has shown that one of possible mechanism of the suppression of the processes is in increasing the barrier height for electrons ΔE_c up to values of order E_g of an active layer.

From physical condition deduced in [23], which declares that if internal quantum efficiency becomes less than 2.5% the obtaining of coherent generation is impossible, we can determine a limit operation temperature of longwavelength lasers :

$$\eta_{int}=I_{thR}/(I_{thR}+I_{thA})=2.5\%$$

This condition takes into account band gap parameters of active layer and confinement layers. They can be chosen to minimise Auger-recombination rates caused by CHHS and CCHC-processes. In our calculation we use the following parameters of our lasers: for $InAs_{1-x}$ Sb_x active layer x=0.055, Eg=0.371eV (λ_{gen}=3.2μm at T=77K), Δ_0=0.408eV, m_e^*=0.023m_o and for confinement layer E_g=0.602eV for InAsSbP layer with P content of content 35%.

We obtained an important result: in such laser structure quantum efficiency can be achieved about 3% at T=250K. It means that in mid-IR lasers based on InAs alloys a lasing can be obtained up to 250K (see calculation curve in Fig.(22)).
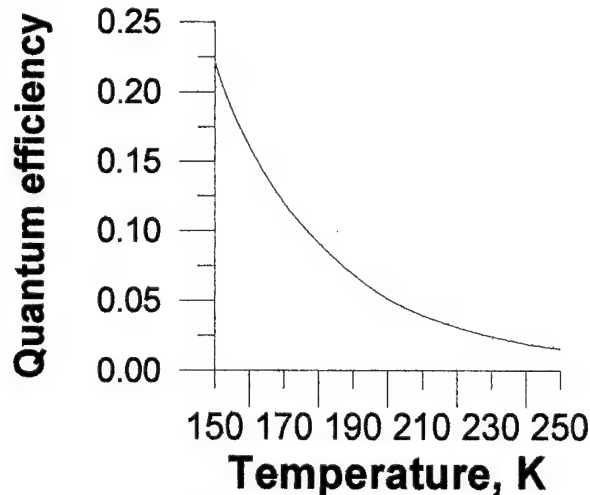
Fig.22. Calculated internal quantum efficiency versus temperature for InAsSb/InAsSbP laser (x=0.055, E_g=0.371 eV, D_o=0.408 eV at T=77K).

Theoretical analyses and experimental studying allow to conclude that for increasing both operating temperature and internal quantum efficiency of longwavelength lasers based on InAs alloys it is need:

1. To suppress of non-radiative CHHS-Auger process due to spin-orbit splitting valence band ($\Delta o/E_g > 1$) as well as CCHC-process.
2. To raise barrier heights of confined layers and decrease intraband absorption at heteroboundary.
3. To decrease leakage currents due to hot Auger-carriers by increasing heights of band-offsets ΔE_c, ΔE_v.

It is preferable to use type-II heteroboundary in an active layer. It may lead to weaker temperature dependence of non-radiative Auger-recombination rate as it was predicted in [28].

III. Creation and studying mid-infrared lasers with strain active layer and improved confinement based on InAsSb/InAsSbP

3a. Theoretical calculation of strained active layer effect on threshold current of InAsSb/InAsSbP double heterostructure lasers.

It is known that in heterostructures with strained layers hole spectrum essentially changes [29]. The main result is in splitting of the light and heavy hole energy bands, and this splitting is proportional to the value of elastic strain [30,31].

In double heterostructure (DH) strain influence threshold characteristics through energy band parameters of the splitting light and heavy hole bands. We studied this influence on the value of the threshold current density and internal quantum efficiency.

As it was shown earlier [25,26] threshold current of the DH lasers is determined by two channels of recombination: radiative recombination and non-radiative Auger. As it was shown for the first time in [27], in DH there are two principally different types of the Auger recombination. The first type is an ordinary threshold mechanism of Auger recombination process in bulk semiconductors. The rate of this process is an exponential function of temperature. Exponential (with threshold energy) Auger recombination rate dependence on temperature is a consequence of two conservation laws: the conservation of energy and the conservation of quasi-momenta of particles participating in the Auger recombination. The second type of the Auger recombination is due to the non-threshold mechanism; a rate of this process is a power function of temperature. The last is the consequence of absence of the conservation law of the momentum component perpendicular to the heteroboundary. For DH with thin active region non-threshold channel is the main process of non-radiative recombination of the carriers.

We studed influence of the elastic strain in DH on the following processes: radiative recombination, bulk (threshold) Auger recombination and non-threshold Auger recombination which is due to the carrier interaction with heteroboundary. It was shown that elastic strain in heterostructures in a greater extent effects on the rate of non-threshold Auger recombination.

For typical values of the lattice constant mismatch we have: $\Delta a_0/a_0 < 1\%$ where $\Delta a_0 = a_0 - a$; a_0 is the bulk lattice constant of InAsSb and a is lattice constant of InAsSbP. Theoretical analysis shows that the ratio between the rates of radiative recombination R_{str} and R calculated with and without taking into account elastic strain respectively is of order of unit: $R_{str}/R \sim 1$. For example, for the structure InAsSb/InAsSbP elastic strain at x=0.13 and $\Delta a/a0 = 0.9\%$ we have: $R_{str}/R = 1.083$.

Finally in DH based on InAsSb/InAssbP elastic strain practically does not effect on the radiative recombination rate. It agrees with experimental data.

For the structure under study InAsSb/InAsSbP with x>5% (when noticeable strain is possible) band gap is less than the spin orbit splitting value Δ_0. Therefore Auger recombination process with transition in spin-orbit splitting valence band (such as CHSS process) are not important for given structures.

Using the same values of parameters as for calculated radiative recombination rate R for evaluation Auger recombination rates CHCC and CLCC processes in strained structures G_{str} and non-strained structures G we have:

$G^{str}_{CHCC}/G_{CHCC}=0.956$,

$G^{str}_{CLCC}/G_{CLCC}=1.67$.

Note that as it is in the case without elastic strain CHCC process dominates over CLCC process, i.e. $G^{str}_{CHCC}>>G^{str}_{CLCC}$.

For strained laser heterostructures analysis of non-threshold processes was fulfilled in detail in [32]. Taking into account interaction of carriers with heteroboundary we will found using results of [32]:

$$\mathbf{G^{str}} = (2\pi)^2 \sqrt{2} \frac{\mathbf{E_B}}{\mathbf{h}} \frac{\mathbf{V}}{\mathbf{E_g}^{hl}} \frac{\mathbf{T}}{\mathbf{E_g}^{hl}} \left(\frac{h^2}{2m_c E_g^{hl}} \right)^{\frac{7}{2}} \frac{1}{2} \mathbf{n^2 p} \qquad (10)$$

where $\mathbf{E_B} = \dfrac{m_c e^4}{2\kappa^2 h^2}$ is Bohr energy,

$$\mathbf{E_g}^{hl} = \mathbf{E_g} + \mathbf{b}\frac{C_{11}+2C_{12}}{C_{11}}\frac{\Delta a_0}{a_0} + 2a\frac{C_{11}-C_{12}}{C_{12}}\frac{\Delta a_0}{a_0} \qquad (11)$$

C_{11}, C_{12} are elastic constants, $\mathbf{n, p}$ are electron and hole concentrations respectively.

For quantitative analysis of strain influence on the rate of non-threshold Auger-recombination channel we employ parameters specified above. We get that ratio of the recombination rates with and without strain G^{str} and G, respectively is $G_{str}/G=1.18$.

From the analysis carried out it follows that elastic strain has insignificantly influence on the Auger-recombination process in double heterostructure lasers. Threshold process rate varies in the smaller extent (on 5%) with strain than non-threshold one (on 18%).

3b. Experimental investigation of the lasers with strain active layer

We also studied experimentally InAsSb/InAsSbP laser structure with slightly strained InAsSb active layers.

With increasing InSb content from 0 to 5.5 % we can see red shift of the emission spectra from 3.016 µm to 3.6 µm. Lattice mismatching changed in this case in the range 0.02 - 0.69 %.
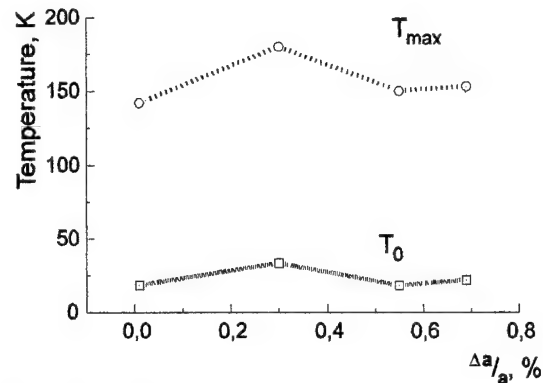

Fig.23. Temperature dependence of T_{max} and characteristic temperature T_0 on lattice-mismatching $\Delta a/a$ of InAsSb active layer and InAs substrate.

Fig.23 represents dependencies of maximal operating temperature T_{max} and characteristic temperature T_0 on lattice-mismatching value $\Delta a/a$. As one can see small lattice mismatching (0.01-0.03 %) leads to higher operating temperature. With $\Delta a/a$ increasing T_0 and T_{max} decrease This fact may be explained by formation of dislocation due to strain.

In our laser structures we used usually active layers with thickness about 0.5-1.5 µm and only in several cases 0.2-0.3 µm. Obtaining thinner active layers by LPE method is a special and non simple task. Appearance of dislocations in our strained structures leads to smoothing of absorption edge.

Taking into account both results of the theoretical calculation and our experimental data we can conclude that strain effects do not influence strongly on performance of our InAsSb/InAsSbP DH lasers due to large thickness active layers (0.5-1.5 µm).

Experimental and theoretical investigations of the recombination processes in DH laser structures of type I and threshold characteristics of heterolasers have shown that the main physical process which restrict high temperature operation of MID-infrared lasers is Auger-recombination process. In structures with thick active region (d>1 µm) at given value of E_g the Auger recombination rate practically does not depend on the parameters of the heterostructures. For the DH lasers with thin active region the rate depends on the active region thickness **d** and on the barrier height for electrons ΔE_c: $G_A \sim \Delta E_c/d$.

In this case the non-radiative recombination rate is a monotonous function of structure parameters. Consequently, possible suppression of the Auger recombination process by variation of parameters of the laser structure based on type-I is not so effective.

More essential decrease of the Auger recombination rate is expected in type-II heterostructures. In [28] it have been shown that mechanism of Auger-recombination in the type-I are principally different from one in type-II heterostructures. Under several conditions suppression of Auger recombination can take place. This fact opens a principle possibility for the creation of mid-infrared lasers operating at room temperature.

The objective of the work fulfilled in the frame of the Proposal was increasing operation temperature InAsSb/InAsSbP lasers in the spectral range 3-3.5 μm. In the frame of the Phase I of the program we created and investigated some designs of the longwavelength lasers:

1. Traditional double-heterostructure lasers InAsSb/InAsSbP with improved confinement layers (3-layers structures) with P content of 31-35%;
2. DH laser structures with slightly strained active layers;
3. InAsSb/InAs/InAsSbP laser structures with separate electron and optical improved confinement (5-layer structures)(SEOC).

In the result we succeeded in obtaining limit operation temperature of our lasers up to T=203 K in pulse regime with 5th-layers structure and 110 K in continuos wave (CW) operation.

Our analysis shows that with using in the laser design two-side improved optical and electron confinement (using burried laser structures, higher barrier confined layers) we can rise operating temperature up to 220-250 K. But further progress in the range of higher temperature mid-infrared lasers operation of will be difficult due to increasing non-radiative Auger recombination processes which dominances at higher temperature in the narrow-gap laser structures as it was shown by our theoretical and experimental studying.

Therefore, we proposed new physical approach to creation of mid-infrared lasers.

We offer to use in the active layer of new laser structure type-II broken-gap isotype p-p heterojunction.

The following part of this Report will be devoted to creation and studying of novel laser structure.

IV. Novel mid-infrared laser structure based on type II broken-gap p-GaInAsSb/p-InAs(InGaAsSb) heterojunction

4.1. Introduction

We present in this Section a new physical approach to design of III-V mid-infrared lasers which can lead to increasing operation temperature of InAs-based lasers. Fundamental feature of this approach is using interface radiative recombination of spatially separated carriers in type II broken-gap p-p heterojunction.

Recently some attempts were made to decrease the contribution of Auger-processes by using both strained active layers and higher cladding ones in narrow-gap laser structures [33-35]. Demand for room temperature operating mid-IR lasers stimulates a search of new alternative heterostructures [36] as well as investigation of new physical mechanisms of the obtaining of coherent generation using non-traditional approaches. So, recently unipolar quantum cascade laser was proposed by Capasso with co-workers [37].

Recently we proposed and realised quantum well laser based on type II staggered heterojunction in the system of GaInAsSb/GaSb with lasing at λ=1.8-2.2μm[38]. In the laser structure radiative recombination occurs through localised states in self-consistent quantum wells in p-n structure by applying forward bias at low temperatures (4.2-77K).

Main features of such quantum well laser were: very low threshold current at low temperature and photon energy values of coherent generation less than energy band gap of the narrow gap GaInAsSb layer.

In the frame of this work novel infrared laser was realised for the spectral range 3-5 μm with using type II broken-gap isotype p-p heterojunction in an active layer.

In type II broken-gap heterojunctions valence band of the wider-gap semiconductors situated above conduction band of the narrow-gap one (e.g. GaSb-InAs HJ [39]). There are closely spacing deep quantum wells for electrons and holes at the interface. By applying external electric field we can change relative position of the bands at the interface as well as carrier population in the quantum wells. Under some conditions it can lead to high probability indirect radiative recombination through the interface in such structures.

We observed of unusual intensive electroluminescence (EL) due to indirect radiation recombination of spatial separated localised electron and holes in type II isotype broken-gap p-GaInAsSb/p-InAs single heterostructures [40,41] and propose a novel laser structure using this effect [42].

4.2. Interface electroluminescence in type II broken-gap p-GaInAsSb/p-InAs single heterostructure.

Consider before an appearance of electroluminiscence at type II broken-gap heterostructure.

Lattice-matched p-GaInAsSb/InAs HJ structures was prepared by LPE. Zn-doped p-GaInAsSb layer with In content of 17% was grown on p-InAs (100) substrate ($p=5\times10^{16}$cm^{-3}) with lattice-matching $\Delta a/a<2\times10^{-4}$. Doping level of p-GaInAsSb layer with 2μm thickness can changed from non-doped up to $p=1\times10^{18}$ cm^{-3}. Energy gap of $GaIn_{0.17}As_{0.22}Sb$ Eg=0.63eV (T=77K) was determined by photoluminescence and photoconductivity. Rough band energy diagram of GaInAsSb/InAs heterojunction was before established by us in [43]. It was shown this structure was type II broken-gap heterojunction with a gap about $\Delta \sim$60-100 meV between valence band of $GaIn_{0.17}AsSb$ and conduction band of InAs.

2D-electron channel with high mobility (u= 70 000 cm^2/ V*s at T=77 K) was observed in p-GaInAsSb/p-InAs structure with undoped quaternary layer. Existence of strong electron channel on the interface of p-GaInAsSb/p-InAs HJ was demonstrated also by scanning electron microscopy (STM) experiment (see Fig.24).
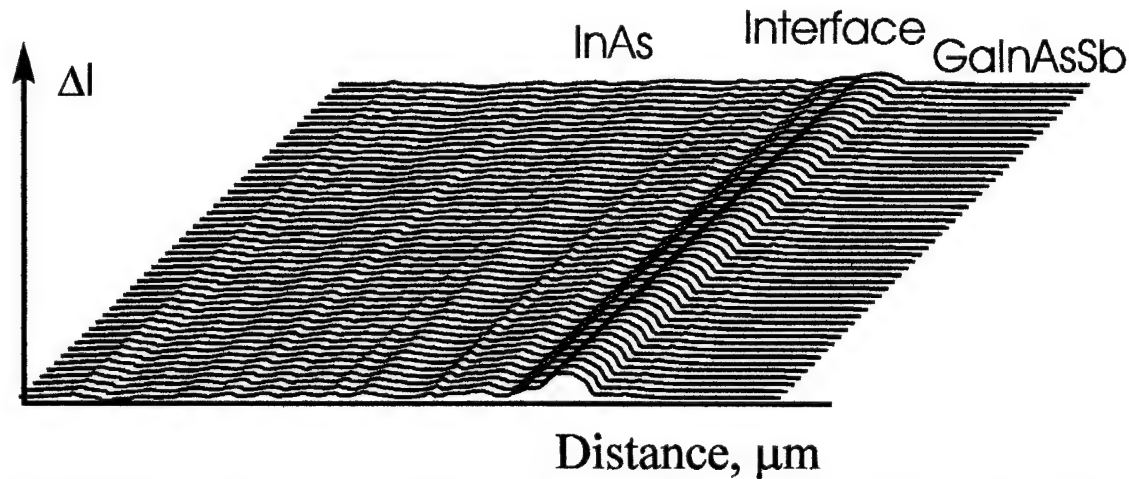
Fig.24. Direct observation of the cleaved surface of the broken-gap type II p-Ga$_{.83}$In$_{.17}$As$_{.22}$Sb$_{.78}$/p-InAs heterojunction in air using current imaging tunneling spectroscopy (CITS). The area scanned is 5μmx5μm. The maximum difference ΔI in the current values on the image surface is 12 nA.

Galvanomagnetic properties and Shubnikov-de-Haas oscillations of longitudinal magnetoresitivity was measured in moderate magnetic fields up to B= 4T at T=1.5-77K (Fig.25). Concentration of 2D-electrons in the channel n_S $=2\times10^{11}$ cm^{-2} and effective mass m=0.026m$_0$ equal to InAs electron effective mass were determined from these experiments. It was an evidence that electron channel with high mobility was situated at InAs-side.

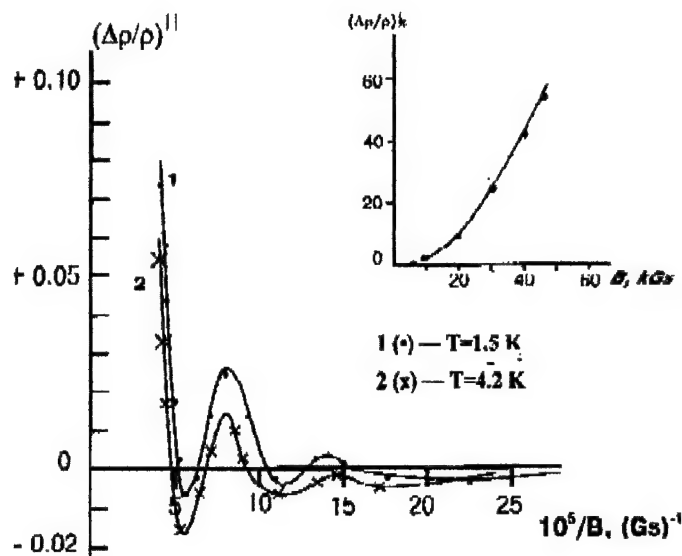Fig.25. Shubnikov de-Haas oscilations at the longitudinal magnetoresistance of p-GaInAsSb/p-InAs heterostructure versus inverse magnetic   field.   1 -T=1.5K,   2 - T=4.2K.   Inset: Transverse magnetoresistance .

Mesa-diodes of 300 µm diameter were prepared by standard photolitography. Ohmic contacts were made by Au:Zn alloy, with point contact to quaternary layer and solid one to substrate. Rectifying current-voltage characteristics were observed in P-p single heterostructures under study. Electroluminescence spectra were measured by grating monochromator of type MDR-4 and registrated by cooling InSb photoconductor using lock-in detection technique.

Intensive electroluminescence with three pronounced emission bands was observed in the spectral range of 3-5 µm at T=77 K at applied bias in the interval from 2 to 4 Volts, with a negative polarity at the narrow-gap semiconductor (InAs). EL spectra of p-GaInAsSb/p-InAs structure are presented in Fig.27. Electroluminescence can be detected beginning from low drive currents (3-5 mA). Two of the emission bands were intensive and very narrow while the third band was more weaker and broader. All bands labelled as 1, 2 and 3 in Fig.27. Related intensity and spectral position of the bands can be changed by drive current. Two peaks 1 and 2 had photon energies of maxima $h\nu_1$= 316 meV and $h\nu_2$= 378 meV with full width at half maximum (FWHM) 20 and 10 meV, respectively. Third broader band was situated at $h\nu_3$= 630 meV and its FWHM was about 60 meV. Photon energy of the narrow peaks shift slightly in short wavelength region with current increasing.

We must note that EL intensity at T=77K obtained in the p-p structures under study was very intensive and comparable with one of conventional p-InAs/n-InAsSbP light-emitting diode operating at room temperature. Significant intensity of EL was observed in our structures up to 300 K.
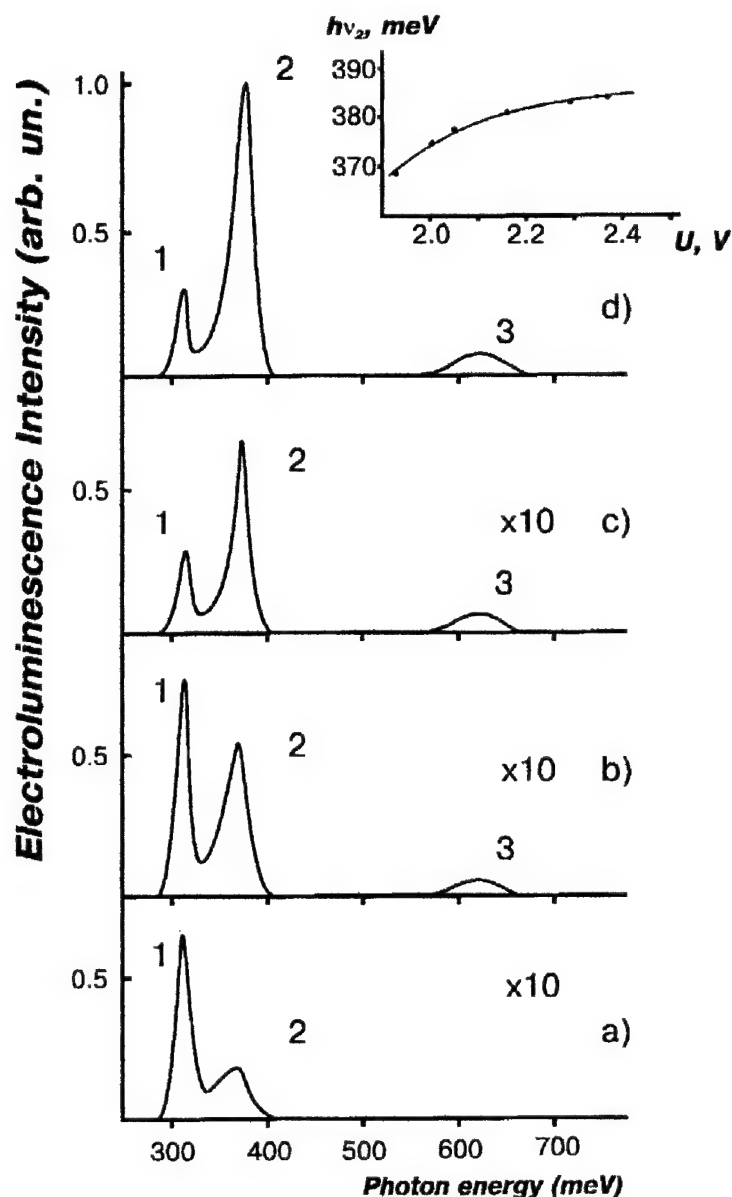
Fig.26.   Electroluminiscence   spectra   of   p-GaIn$_{0.17}$AsSb/p-InAs heterojunction   under reverse applied bias, negative potential at p-InAs substrate.   T=77K. DC drive current, mA: a)-20, b)-50, c)-100, d)-120.
Inset: Shift of photon energy of EL band hv$_2$ versus applied bias.

Intensity of the broader emission band 3 changes weakly with drive current and maximum optical power of the band 3 was also lower in order to ten in comparing with the narrow band 1 and 2. With current increasing at first band 1 appears, and then, with current value i >20 mA, band 2 arises (see Fig.26).
Intensity-current dependence at low currents can be described as I ~ i^3, and with current increasing (i>20mA) as I~i (Fig.27a). With temperature increase T>77K photon energy maxima of bands hv$_1$ and hv$_2$ move in the longwavelength region,

and at high temperature (200-300 K) there is only one emission band $h\nu_2$ in EL spectrum. Intensity of electroluminescence decreased about in 25 times in the range of 77-300 K (See Fig.27b).
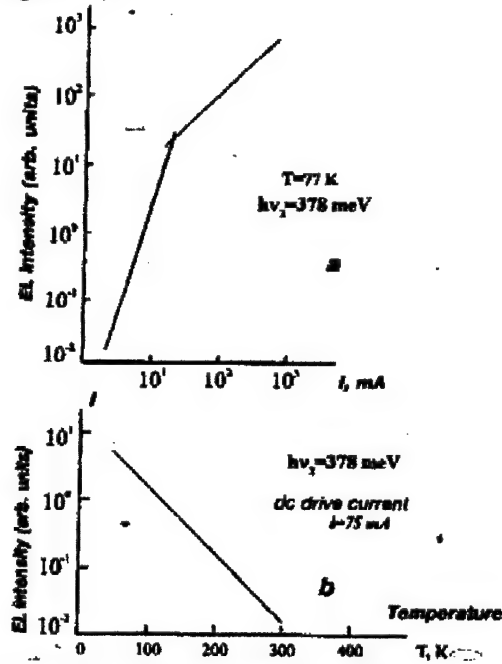
Fig.27. a. Maximum intensity of emission band $h\nu_2$ versus drive current.
b. Relative intensity of peak 1 (I_1) depending on drive current. T=77K.
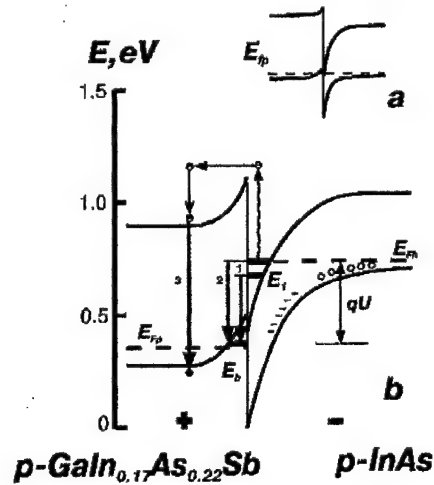
Fig.28. Energy band diagram of p-GaInAsSb/p-InAs heterojunction under zero bias (a) and 'reverse" applied bias (b). E_1,E_2, E_h are electron and hole levels in the quantum wells E_F, E_{Fp} are Fermi quasi-leves, U is applied voltage, Arrows show possible radiative recombination transitions corresponding to the emission peaks 1,2,3 in Fig.26. Wavelike line shows an eiection of Auger-electtron into wide-gap GaInAsSb layer.

To analyse the experimental results let us consider energy band scheme of the p-GaInAsSb/p-InAs heterostructure at zero bias and under applied bias (See Fig.28) and explain an appearance of electrons in isotype p-p heterostructure.

2D-electron gas can appear in the quantum wells near the interface of p-p type II broken-gap HJ at the side of narrow-gap semiconductor due to electron transfer (at zero bias) from valence band of wide-gap material to conduction band of narrow-gap one [9]. By applying external electric field with a negative potential to the narrow-gap semiconductor energy bands at the interface displace against each other in such a way that conduction and valence bands of the narrow-gap semiconductor and of wide-gap one move up and down, respectively. By such condition electron from acceptor levels of slightly-doped p-InAs can resonance tunnel to 2D-electron channel when Fermi quasi-level crossed electron levels in the quantum wells near the interface. As a result non-equilibrium electrons and holes which are localised at the different sides of the interface can effectively recombine due to mutual tunnelling through the interface.

Narrow emission peaks observed in our structure are connected with the electron transitions from discrete levels E_1 and E_2 in quantum wells and their radiative recombination with holes confined in the wide-gap material. Possible recombination transitions are labelled by arrows 1, 2, 3 (as in Fig.28). The experimental distance between two narrow luminescent peaks 1 and 2 in Fig.26 is ΔE_{12}= 62 meV and corresponds to energy difference between E_1 and E_2 level. From this value and knowing energy positions of the peaks we can obtain energy position of 2D-electron levels E_1=210 and E_2=270 meV in quantum well at the side of InAs.

We can also calculate two-dimensional electron concentration in structure under external field from the condition E_F=E_2, when Fermi quasi level E_F crosses discrete electron level E_2. We found n_s=1* 10^{12} cm^{-2} .

As to a broader emission band 3 observed in EL spectra (Fig.26) hv_3=0.63eV (this energy equal to E_g of quaternary GaInAsSb layer), it can be explained by recombination of ejective Auger-electrons with bulk holes in the flatten-band region of wide-gap semiconductor (See wave-like line in Fig.28).

4.3. Novel tunnel-injection laser structure based on type II broken-gap p-p heterojunction.

Observed effect of striking intensive interface electroluminescence under tunnel injection of electrons (at applied bias of proper polarity) was used by us for designing novel laser structure.

Laser structure contained 6 layers (see Fig.29) predominantly of p-type conductivity was grown LPE on p-InAs (100) substrate. In active layer of the laser type II broken-gap p-p heterojunction was grown formed by two quaternary layers: wide-gap $GaIn_{0.17}As_{0.22}Sb$ (E_g=0.63 eV at T=77 K) layers by thickness 2 μm and narrow-gap $GaIn_{0.83}As_{0.80}Sb$ layers (E_g=0.39 eV at T=77 K), with thickness about 0.8 μm. For improving electron and optical confinement we used wide-gap quaternaries GaInAsSb and InAsSbP as cladding layers because it allows us to obtain a big difference of refractive indices between an active region and cladding

layers ($\Delta n \cong 0.2$). Thickness of InAsSbP (P~0.26) layer was about 1.7 μm. P-n junction was situated in the wide-gap cladding GaInAsSb layer (E_g=0.63 eV) and it was intend for additional electron injection into quantum well of broken-gap structure. As a cap layer n^+-InAs was used.

Mesa stripe lasers were fabricated by standard photolithography with stripe width of 60 μm and cavity length of 350 μm. Contacts were made by evaporation of Au:Zn alloy (to p-material) and Au:Te (to n-material) and then were fused at H_2 atmosphere.

Fig.30 represents spectrum of spontaneous emission of novel laser structure at T=77K. There are two intensive emission bands 1 and 2 in the spectral range 3-4μm like it was observed in EL spectra of single p-p heterostructure (see Fig.26).
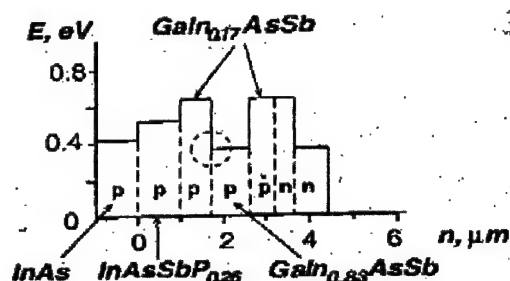
Fig.29. Novel laser structure with type II broken-gap p-p heterojunction in an active layer.

Coherent emission arises at shortwavelength edge of spontaneous emission band 2, unlike traditional laser structures.

Single-mode coherent emission was observed at λ=3.26 μm at T=77 K (see Fig. 31.). Threshold current density was about 2 kA/cm^2 in pulse regime.

Fig.30. Electroluminiscence spectrum of p-GaInAsSb/p-InAs single heterojunction at **dc** drive current I=100mA. T=77K. Emission bands 1 and 2 (see text).

Fig.31. Single-mode lasing of laser structure shown in Fig.29. T=77K. Pulse regime. I_{th}=2 kA/cm^2

A very important fact was the weak temperature dependence of threshold current (Fig.32) and high value of characteristic temperature up to T_0=40-60 K

Fig.32. Temperature dependence of threshold current for novel laser structure.

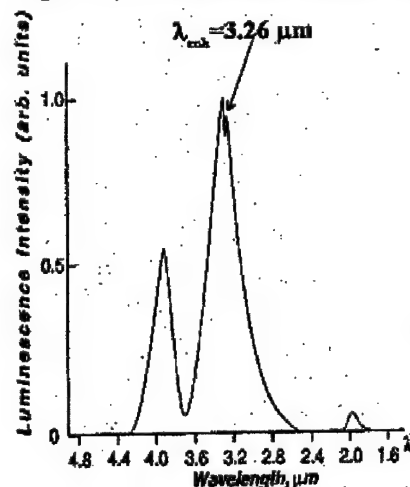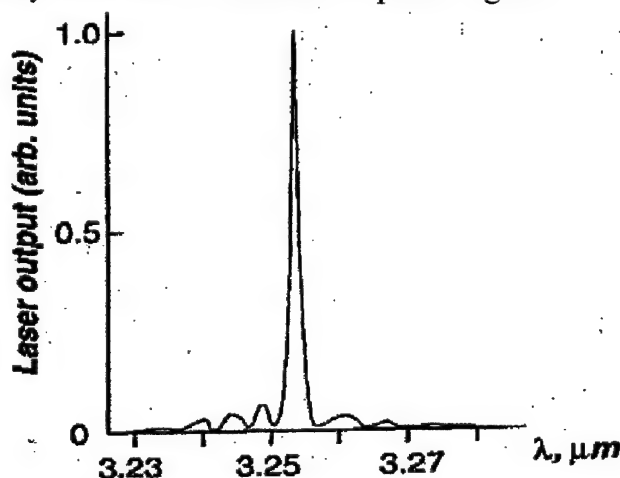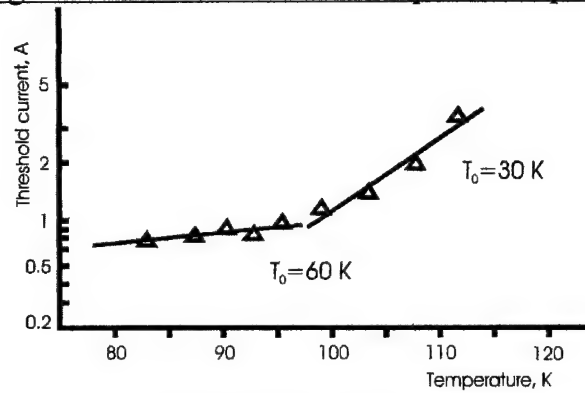which was found for our novel laser structure in the range of 77-110 K. This T_0 value is the highest one for InAs-based lasers described before [9, 17].

It is need to note that threshold current density in these first novel laser structure was higher in comparing with our InAsSb/InAsSbP DH lasers which was described in Section II.

Main advantage of novel laser structure is using interface tunnel radiative recombination at type II broken-gap heterojunction. As it was shown in [28] non-radiative Auger-recombination can be suppressed at type II heteroboundary. In our case of interface recombination we exclude also "resonant" Auger-process (CHHS) connected with spin-orbit splitting of valence band ($E_g{\sim}\Delta_0$) which contributes in bulk narrow-gap p-semiconductors [12,13].

Investigation of threshold current density dependence shows that in the range 77-120K there are two various parts of this curve: at low temperature (T<100K) I_{th} depends weakly on T (so-called characteristic temperature can be evaluated as $T_0{\sim}$40-60K), and at T>100K I_{th} is more sharp function of temperature (here $T_0{\sim}$26-30K). It is obviously that such behaviour of threshold current determined by two recombination mechanisms: radiative recombination and non-radiative Auger recombination G. We calculated temperature dependence of threshold current taking into account both recombination processes: $\mathbf{I_{th}=e(R+G)}$.

In the type II heterostructure under study radiative recombination (unlike traditional type I double heterostructure) can be realised by two channels (See band energy diagram for type II heterojunction in Fig.28):

i) electron can tunnel through the heterobarrier and recombine with hole:

ii) hole can tunnel through the barrier and recombine with electron in the quantum well of narrow gap semiconductor.

Our estimation shown that the first channel prevails in the case of p-p-heterostructure under study.

Temperature dependence of radiative recombination rate is described by the following equation:

$$R \approx \frac{\pi}{2} \frac{\varepsilon_\infty}{\sqrt{\kappa_0}} \frac{e^2}{\hbar c} \frac{E_g^*}{\hbar} \frac{E_g^*}{m_c c^2} \frac{\hbar^2}{2m_c \Delta E_c} \frac{m_h}{m_c} \frac{T}{\Delta E_c} np \qquad (12)$$

Here ε_∞, ε_0 are static and high frequency dielectric constant, E_g^* is effective energy gap equal toenergy distance between discrete levels of electron and hole, m_c, m_h are effective mass of electrons and holes, ΔE_c is heterobarrier height for electrons, n, p are two-dimentional concentrations. As it can see from (13) temperature dependence of the radiative threshold current will be proportional to $I_{th} \sim T$. As it was shown in [28], matrix element of non-radiative Auger recombination transition in type II heterostructures unlike one in type I heterojunction has an additional infinitesimal $\left(\dfrac{T}{\Delta E_c} \dfrac{m_h}{m_c} \right) \ll 1.$ \qquad (13)

Due to a ratio of Auger-recombination rates type II and type I heterostructures can be evaluated as:

$$\frac{G^{II}}{G^I} \sim \left(\frac{T}{\Delta E_c} \frac{m_h}{m_c} \right)^2, \qquad (14)$$

and using parameters of heterostructure under study $\Delta E_c = 400 meV$, $m_c = 0.023 m_0$, $T \sim 100K$, we obtain $G^{II}/G^I \sim 0.15$. Auger-recombination rate depends on temperature as $G^{II} \sim T^2$ or $\sim T^{5/2}$ (in dependence on structure parameters) as it was found [?].

Therefore one of main advantages of novel laser structure with an type II heterojunctions in an active layer is suppression of Auger-recombination process on the heteroboundary and weakening its temperature dependence in comparing with laser structure based on type I heterojunctions. Besides this situation leads also to increasing quantum efficiency.

Now we are going to work on improving both technology and design of our new laser structures. We hope to decrease threshold current density and increase operating temperature of these lasers.

Novel physical approach to design a laser structure whith was proposed and realised in the frame of this work allows to conclude that this is open the way of creation high efficiency mid-infrared lasers operating at higher temperature up to near-room temperature.

CONCLUSION

1. Technology of the laser structures based on InAs/InAsSb/InAsSbP type I heterostructures was developed. Double heterostructure lasers as well as laser structures with separate electron and optical confinement were made and investigated.

1.1. InAsSbP solid solutions with the compositions near immiscibility gap was grown with Phosporous content of 31-35% for improving cladding layers.

1.2. Unique method was developed to determine a position of heterointerface and p-n junction by using scanning electron beam.

2. Theoretical and experimental studying of threshold current of the laser structures depending on the temperature were carried out with taken into account contributions of radiative and non-radiative (Auger) recombination processes.

2.1. It was shown that in the region of low tempertaures (T<100 K) radiative recombination dominanted in the threshold current of the lasers under study. At higher temperature in the range 100-250 K threshold current is determined by two compete recombination processes: with participating the conduction band (CCHC-process) and the spin-orbit splitting valence band (CHHS - process).

2.2. High operating temperature T=203 K was achieved in pulse regime in InAsSb/InAsSbP laser structure with separate optical and electron confinement. Single mode cw operation was obtained up to T=110 K.

2.3. It was found by theoretical calculation that quantum efficiency for coherent emission of InAsSb/InAsSbP DH laser structure decreased from 25 to 3.5% in the temperature range 150-250 K. It is evidence a potential opportunity to get in our lasers coherent generation up to 250 K. Main physical causes limiting operation of middle-infrared lasers at higher temperatures were considered.

3. Strain affect on threshold current of InAsSb/InAsSbP laser structures was studied both theoretically and experimentally. It was established that strained active layers in the lasers under study do not influence noticable on the threshold currents.

4. New physical approach was developed to creation of the middle infrared lasers.

Novel tunnel injection laser based on type II broken gap isotype p-p single heterojunction was proposed and realised.

In this laser structures with p-GaInAsSb/p-InAs (InGaAsSb) active layer intensive spontaneous and coherent emission was achieved due to indirect tunnel radiative recombination of spatially separation electrons and holes confined in the quantum wells at different sides of the heteroboundary.

Theoretically predicted and experimentally observed non-radiative Auger recombination process suppression and its temperature dependence weaking at type II heteroboundary.

High characterisctic temperature T_0=40-60 K was achieved in the range of 77-120 K.

These results open the way to increase operation temperature of middle infrared lasers up to room temperature.

Further work on the creation of middle infrared lasers operating near room temperature by our opinion must be in the following main directions:

i) Improving traditional lasers based on the InAs/InAsSb/InAsSbP heterostructures by using burried laser structures with two-side confinement. It can lead to eliminate surface leakage. It permits to increase operating temperature up to 220-250K. Such lasers with thermoelectrical cooling are very promissing for high resolution laser diode spectroscopy and ecologycal monitoring.

ii) Another way consists in futher studying and improving design of the new tunnel injection laser based on type II broken gap heterostructure.

REFERENCES

1. A.I.Nadezdinsky, A.M.Prokhorov in : SPIE, 1724, Tunable Diode laser Applications, 1992, 2-64.
2. A.I.Kuznetsov, A.I.Nadezhdinsky et al., ibid 104-108.
3. E.A.Bochkarev, L.M.Dolginov, A.E.Drakin, L.V.Druzhinina, P.G.Eliseev, B.N.Sverdlov, V.A.Skripkin, Sov.J.Quant.Electron., 1986, 16, 1397.
4. J.L.Zyskind, J.C.ReWinter, G.A.Burrus, J.C.Centanni, A.G.Dentai and M.A.Pollack. Electr.Lett., 1989, 25, 568.
5. H.K.Choi, S.J.Eglash. IEEE J. Quant.Electr., 27 ,1555 (1991).
6. A.P.Shotov. SPIE, 1724, 1992, 64-77.
7. A.N.Baranov, E.A.Grebenshikova, B.E.Dzurtanov, T.N.Danilova, A.N.Imenkov, Yu.P.Yakovlev. Sov.Tech.Phys.Lett., 14(10), 1988.
8. N.Kobayashi, J.Horikoshi. Jpn.J.Appl.Phys. 19, L641 (1980).
9. M.Aidaraliev, N.V.Zotova, S.A.Karandashev et al., Phys.Stat.Sol.(a), 115, K117 (1989).
10. H.Mani, A.Joullie, G.Boissier et al. Electron.Lett., 24(25) 1988, 1542-1543.
11. H.K.Choi, S.J.Eaglash. The conf. LEOS san Jose, CA, Nov. 4-7, 1991, paper SDL6.2.
12. M.P.Mikhailova, A.A.Rogachev, I.N.Yassievich. Sov.Phys.Semicond., 10(8), p.460 (1976).
13. B.L.Gelmont, Z.N.Sokolova, I.N.Yassievich, Sov.Phys.Semicond., 16, 382-387 (1982).
14. M.P.Mikhailova, D.N.Nasledov et al. Fiz. I Techn. Poluprovodnikov, 3, 1973.
15. M.Aidaraliev, N.V.Zotova, S.A.Karandashev et al., Pisma v Zh.Techn.Fiz. (Sov. Phys. Tech. Lett.), 15(15), 49-52(1989).
16. H.K.Choi, S.J.Eaglash. Appl.Phys.Lett.,61, 1154(1992).
17. A.N.Baranov, A.N.Imenkov, V.V.Sherstnev, Yu.P.Yakovlev. Appl.Phys.Lett., 64(19), p.2480-82 (1994).
18. A.M.Litvak, N.A.Charykov , Zhurnal Physicheskoii Khimii (J. Of Phys. Chem.), v.64, No.9, 2331 (1990).
19. A.N.Baranov, B.E.Dzhurtanov, A.M.Litvak et al., , Zhurnal Neorganicheskoii Khimii (J. Of Inorganic Chem.), v.35, No.12, (1990).
20. A.N.Baranov, A.M.Litvak, K.D.Moiseev, N.A.Charykov, V.V.Sherstnev, Zhurnal Physicheskoii Khimii (J. Of Phys. Chem.), v.64, No.7, 1651 (1990).
21. E.R.Gerner, D.T.Cheng, A.M.Andrews, J.T.Longo, J. Electron Mat., v.6, No.2, 163 (1977).
22. V.A.Solov'ev, S.A.Solov'ev, V.E.Umansky, Izvestia Academii Nauk, sec. Fiz., v.54, No.2, 232-236, (1990).
23. J.Horikoshi in book: Semiconductors and Semimetals. Academy Press, N.Y., 1985, v.22 pp.93-147.

24. M.Sh.Aidaraliev, G.G.Zegrya, N.V.Zotova et al., Sov-Phys. Semicond. 26(2), 138 (1992).
25. A.A.Andaspaeva, A.N.Baranov, B.L.Gelmont, B.E.Dzhurtanov, G.G.Zegrya. A.N.Imenkov, Yu.P.Yakovlev, S.G.Yastrebov, Sov. Phys. Semicond. V. 25, 240 (1990).
26. A.P.Dmitriev, M.P.Mikhailova, I.N.Yassievich, Phys. Stat. Sol., (6), 140, 9, (1987).
27. G.G.Zegrya, V.A.Charchenko, Sov. Phys., JETP, 48, 268 (1992).
28. G.G.Zegrya, A.D.Andreev in book: Nanostructure 95: Physics and Tecnology, Abstr. Of Invited Lectures and Contributed Papers, St.Petersburg, Russia, 26-30 June, 1995, p.163-166.
29. B.K.Ridly, J. Appl. Phys. 68, 4667 (1990).
30. E.Yablonovich and E.O.Kane, IEE J. Lightwave Technol., LT-4, 504, (1986).
31. A.R.Adams, Electr.Lett., 22, 249 (1986).
32. A.D.Andreev, G.G.Zegrya, JETP Lett., 67, (1995).
33. S.R.Kurtz, R.M.Biefield, L.R.Dawson, K.C.Baucom, A.J.Howard, Appl. Phys. Lett., 64, 8/2 (1994).
34. H.K.Choi, G.W.Turner, Appl. Phys Lett. 65, 2251 (1994).
35. Z.L.Liau, H.K.Choi, Appl. Phys. Lett, 64, 3219 (1994).
36. J.H.Zhang, Appl. Phys. Lett, 66, 3219 (1995).
37. J.Faist, F.Capasso, D.L.Sivco, C.Sitrori, A.L.Hutchinson, A.Y.Cho, El.Lett., v.30, No.11,865 (1994).
38. A.N.Baranov, B.E.Dzhurtanov, A.N.Imenkov, A.A.Rogachev, Yu.M.Shernyakov, Yu.P.Yakovlev, Sov. Phys. Semicond., 20, 1385 (1986).
39. L.L.Chang, L.Esaki, Surf. Sci., 98, 70 (1980).
40. M.P.Mikhailova, G.G.Zegrya, K.D.Moiseev, O.G.Ershov, I.A.Andreev, Yu.P.Yakovlev, SPIE, Vol. 2397, p.166-171, (1995).
41. M.P.Mikhailova, G.G.Zegria, K.D.Moiseev, I.N.Timchenko, Yu.P.Yakovlev, Semiconductors v.29, No.4, p.357-361 (1995).
42. K.D.Moiseev, M.P.Mikhailova, O.G.Ershov, G.G.Zegrya, Yu.P.Yakovlev, Pis'ma v Zhurnal Tekhnicheskoii Fiziki (Technical Lett.), v.21, (12), 83 (1995).
43. M.P.Mikhailova, I.A.Andreev, K.D.Moiseev, I.N.Timchenko, Yu.P.Yakovlev, Nanostructures: Physics and Technology, Int Symp., St.Petersburg, Russia, 20-24 June 1994, Abstracts of Invited Lectures and Contributed Papers, p.82.
44. B.L.Gelmont, Z.N.Sokolova, I.N.Yassievich, Sov. Phys. Semicond., 16, (1982).G.G.Zegria, A.D.Andreev, Appl. Phys. Lett. (To be published).

List of publications in the frame of this project:

1. M.P.Mikhailova, G.G.Zegria, K.D.Moiseev and Yu.P.Yakovlev "Electroluminescence of confined carriers in type II broken-gap p-GaInAsSb/p-InAs single heterojunction", SPIE, vol.2397, p.166-171,(1995).
2. T.N.Danilova, O.G.Ershov, G.G.Zegrya, A.N.Imenkov, M.V.Stepanov, V.V.Sherstnev, Yu.P.Yakovlev, "Polarization of radiation of InAsSb/InAsSbP DH lasers", Fizika i Tekhnika Poluprovodnikov (Semiconductors), v.29, N.9, 68-73 (1995).
3. T.N.Danilova, O.G.Ershov, A.N.Imenkov, M.V.Stepanov, V.V.Sherstnev, Yu.P.Yakovlev, "Maximum operation temperature of InAsSb/InAsSbP diode lasers", Fizika i Tekhnika Poluprovodnikov (in print).
4. K.D.Moiseev, M.P.Mikhailova, O.G.Ershov, Yu.P.Yakovlev "Longwavelength laser (λ=3.26μm) with type II broken-gap single heterojunction in an active layer", Pis'ma v Zhurnal Tekhnicheskoii Fiziki (Technical Lett.), v.21, N.12, 83 (1995).
5. K.D.Moiseev, M.P.Mikhailova, O.G.Ershov, Yu.P.Yakovlev "Tunnel-injection laser based on type II broken-gap single heterojunction", Fizika i Tekhnika Poluprovodnikov (Semiconductors), v.29, in print.
6. G.G.Zegrya, A.D.Andreev, , ", Pis'ma v Zhurnal Experimentalnoii i Tekhnicheskoii Fiziki (JETP Lett.), v.67, 749-755 (1995).
7. G.G.Zegrya, A.D.Andreev, "Theory of the excess carrier recombination processes in heterostructures of type II ", in book: Nanostructure'95: Physics and Technology, Abstracts of Invited Lectures and Contributed Papers, 26-30 June, 1995, St.Petersburg, Russia, p. 163-166.
8. Yu.P.Yakovlev, K.D.Moiseev, M.P.Mikhailova, O.G.Ershov, G.G.Zegrya "Tunnel-injection laser based on type II broken-gap p-GaInAsSb/p-InAs single heterojunction", ibid, 329-331
9. G.G.Zegrya, A.D.Andreev, "Suppression of Auger recombination", Appl. Phys. Lett., (to be published).

Main results were or will be reported on the Conferences:

1. Photonic West'95, 4-10 February 1995, San Jose, Califirnia.
2. Nanostructure'95: Physics and Technology, 26-30 June, 1995, St.Petersburg, Russia.
3. International Conference on Semiconductor Lasers: Advanced Materials and Applications, 21-23 August, 1995, Keystone Resort, Keystone, Colorado.
4. 1995 International Semiconductor Device Research Symposium (ISDRS), 6-8 December, 1995, Ohmni Charlottesville Hotel, Charlottesville, VA 22901, USA.